THE HONG KONG POLYTECHNIC UNIVERSITY
香港理工大學

ÉCOLE POLYTECHNIQUE FÉDÉRALE DE LAUSANNE

Working paper

A macroscopic loading model for dynamic, anisotropic and congested pedestrian flows

Flurin S. Hänseler[*,†] William H.K. Lam[†]
Michel Bierlaire[*] Riccardo Scarinci[*] Gael Lederrey[*]

March 23, 2015

Abstract

A dynamic network loading model applicable to anisotropic, time-varying and congested pedestrian flows is proposed. The model is formulated at the aggregate level with respect to time, space and pedestrians. Space is partitioned into cells, each associated with a set of prevalent walking directions. These uni-directional pedestrian streams are represented by links that interact unless pedestrian density is low.

The mathematical formulation of the model is based on a generalization of the cell-transmission model and the underlying LWR theory for traffic flow. It makes use of a recently proposed stream-based pedestrian fundamental diagram that empirically relates density and walking speed for multi-directional pedestrian flows.

[*]Transport and Mobility Laboratory, School of Architecture, Civil and Environmental Engineering, École Polytechnique Fédérale de Lausanne, Switzerland

[†]Department of Civil and Environmental Engineering, The Hong Kong Polytechnic University, Hung Hom, Kowloon, Hong Kong, China

Besides presenting and motivating the proposed loading model, several test cases are discussed that illustrate the behavior of the model in different situations[1]. Particular emphasis is thereby given to the study of test cases involving multi-directional flow. A comparison to a related isotropic loading model allows to assess the advantages of the multi-directional formulation in terms of accuracy and realism. Moreover, a real test case is considered to calibrate the model and to assess its ability to reproduce empirical results.

1 Introduction

Transit systems around the world are facing tremendous, often two-digit annual growth rates in ridership (Kallas; 2014). One of the many consequences of growing demand is that pedestrian areas in transportation hubs are increasingly congested, particularly during peak periods. To mitigate this trend, there is a general need to better understand pedestrian dynamics in these facilities.

Such knowledge may be gained through the development of dynamic traffic assignment (DTA) models. These models are useful for estimating demand (Hänseler et al.; 2015), assessing level of service (Kaakai et al.; 2007), and for crowd control (Seer et al.; 2008).

A DTA model essentially consists of two parts, namely a route choice framework, and a dynamic network loading model (DNL). To this date, several route choice models applicable to pedestrian flows have been developed (Hoogendoorn and Bovy; 2004; Abdelghany et al.; 2012), including specific models for railway stations (Cheung and Lam; 1998; Daamen et al.; 2005). Similarly, a large variety of pedestrian propagation models have been proposed (e.g. Helbing and Molnár; 1995; Blue and Adler; 2001; Hughes; 2002; Robin et al.; 2009). A few of them consider again the specific case of a railway station (Lee et al.; 2001; Daamen; 2004). In spite of these developments, however, there seems to be a lack of pedestrian DNL models that are at the same time behaviorally accurate and computationally efficient (Duives et al.; 2013).

[1]The current version of the manuscript contains only a description of the mathematical model. The discussion of test cases, a case study, as well as a detailed sensitivity analysis is left for the final conference submission.

In an attempt to bridge this gap, several researchers have proposed the use of cell transmission models (CTM) to study pedestrian flows (Asano et al.; 2007; Guo et al.; 2011; Hänseler et al.; 2014). CTM (Daganzo; 1994, 1995) represents a widely used approximation to the LWR theory for car traffic on uni-directional highways (Lighthill and Whitham; 1955; Richards; 1956) that is known for its accuracy and low computational cost.

Representing an inherently isotropic approach, it may be argued that none of the CTMs developed so far sufficiently considers the multi-directional character that is innate to pedestrian flow. Indeed, empirical evidence suggests that in many cases of multi-directional flow the assumption of anisotropy does not hold. Speeds of pedestrian streams moving in different directions may be different, i.e., they may depend both on the flow ratio and on the intersection angle (Lam et al.; 2002; Wong et al.; 2010). Yet the successful application of CTM in various domains related to traffic flow, its low computational cost, and the ease of calibration due to its reliance on a pedestrian fundamental diagram seem to justify a further consideration as a pedestrian propagation model.

To explicitly model multi-directional flow at the macroscopic level, an anisotropic density-speed relation may be used. Recently, Wong et al. (2010) have proposed a corresponding model for bi-directional pedestrian flow, taking into account the flow ratio and intersecting angle. Their work has been further developed by Xie and Wong (2014), who generalize the framework to a n-dimensional pedestrian stream model, i.e., a pedestrian fundamental diagram that explicitly considers the joint presence of n distinct, uni-directional streams. Previous to their work, Weidmann (1992) had already quantitatively discussed the influence of flow ratio and flow pattern on walking speed, however without providing an actual formulation of a multi-directional fundamental diagram.

In this work, we aim to overcome the assumption of isotropy present in pedestrian CTMs proposed so far by developing a cell- *and* link-based DNL that explicitly takes into account the interaction between multiple pedestrian streams. Our approach is inspired by the continuum theory for pedestrian flow (Hughes; 2002) and the stream-based formulation of a pedestrian fundamental diagram developed by Wong et al. (2010) and Xie and Wong (2014). The proposed model is based on a heuristic, multi-directional discretization scheme that is related to Daganzo's CTM as well as a link transmission model (Yperman; 2007) that represents an alternative

discretization of the underlying LWR theory.

2 Model framework

The proposed pedestrian DNL operates in discrete time and discrete space. The temporal discretization is uniform, i.e., each time interval $\tau \in \mathcal{T}$ is of length ΔT.

Walkable space is partitioned into a connected set of cells $\mathcal{X}$. The surface size of a cell $\xi \in \mathcal{X}$ is denoted by A_ξ, which, besides the cell geometry, also takes into account a potential presence of internal obstacles. No a priori assumptions about the shape and size of cells are necessary, except that they have to be convex.

Adjacent cells are connected through gates $\gamma \in \Gamma$, where Γ represents the ensemble of all gates. Cells are considered adjacent if they share a cell edge. Gates have no physical length and act merely as a flow exchange medium.

Within any cell $\xi \in \mathcal{X}$, it is assumed that the prevailing pedestrian flow pattern can be decomposed into a set of pedestrian streams Σ_ξ (Wong et al.; 2010; Xie and Wong; 2014). The set of streams in all cells is denoted by Σ. Each of these streams $\sigma \in \Sigma$ is characterized by a distinct direction of flow. In principle, an arbitrary number of streams may be present in any cell, each representing a uni-directional flow. Cells can be seen as defining an 'area of interaction', in which local streams interfere.

Each stream σ is represented by one or several directed links $\lambda \in \Lambda_\sigma$, where Λ_σ denotes the set of links associated with stream σ. Any link λ has a fixed length $L_\lambda > 0$. The set of links in cell ξ is denoted by Λ_ξ, and the set of all links by Λ.

Fig. 1 illustrates the proposed space representation at the example of a longitudinal corridor and a triangular space discretization. Accordingly, gates can be seen as inter-cell connectors, and links as intra-cell connectors, essentially connecting the gates. The network of cells may be represented by a directed graph $\mathcal{G}_\mathcal{X} = (\mathcal{X}, \Gamma)$ and that of the links by $\mathcal{G}_\Lambda = (\Gamma, \Lambda)$. The combined graph, considering both cells and links, may be denoted by $\mathcal{G} = (\mathcal{X}, \Gamma, \Lambda)$.

To formalize the notion of pedestrian demand, an additional 'higher' level of discretization besides that of cells is introduced. Let an area r

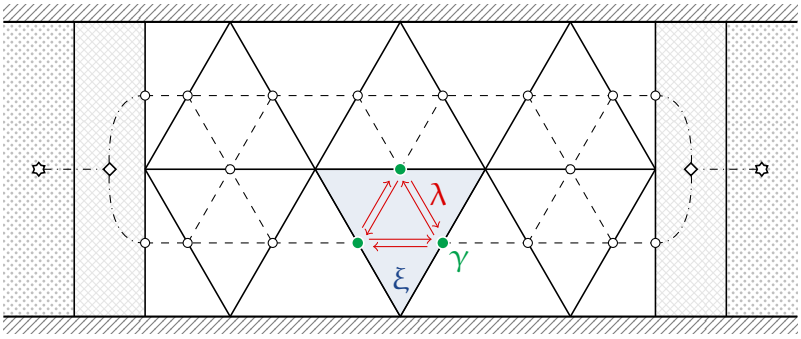

Figure 1: Illustration of space representation at the example of a longitudinal corridor. Space is partitioned into a set of cells $\mathcal{X}$ (one cell is shaded in light blue). Each cell $\xi \in \mathcal{X}$ is associated with a set of prevalent streams Σ_ξ, where each stream σ represents a distinct, uni-directional flow (not shown). Each stream σ is associated with a set of links Λ_σ, on which pedestrians are propagated (denoted by red arrows in the shaded cell, and by dashed lines elsewhere). Adjacent cells are connected through gates $\gamma \in \Gamma$ (denoted by solid green and black dots, respectively). Without loss of generality, in this illustration a triangular grid is used. Source and sink cells at both ends of the corridor are discernible by the star-shaped centroids they contain, and the adjacent auxiliary cells are marked by diamond-shaped nodes.

represent a non-empty and connected subgraph of $\mathcal{G}_\mathcal{X}$, i.e., a connected set of cells (Hänseler et al.; 2014). A pedestrian route may then be defined as a connected set of such areas, $\rho = (r_1, r_2, \dots)$ with origin area $r_o \in \rho$ and destination area $r_d \in \rho$. The ensemble of routes is denoted by $\mathcal{R}$. The origin and destination areas are assumed to consist of a single cell. These cells are adjacent to exactly one 'auxiliary cell', that themselves may be connected to an arbitrary number of cells (in Daganzo; 1995, these cells are referred to as input/output and gate cells, respectively). Fig. 1 illustrates the role of the origin/destination areas as well as of the auxiliary cells.

The set of links emanating from gate γ associated with route ρ is denoted by $\mathcal{O}^\rho_\gamma$, and that of the corresponding links terminating in the same node by $\mathcal{I}^\rho_\gamma$. Moreover, Θ^ρ_λ denotes the set of links that are downstream adjacent to link λ and part of route ρ, and Φ^ρ_λ that of the corresponding links that are upstream adjacent.

The ensemble of pedestrians embarking on a route ρ_ℓ during time interval τ_ℓ is referred to as a pedestrian group ℓ. The set of all pedestrian groups is denoted by $\mathcal{L} \subset \mathcal{R} \times \mathcal{T}$. The size X_ℓ of each group $\ell \in \mathcal{L}$ is assumed to

be known a priori, and the corresponding demand vector is denoted by $\mathbf{X} = [X_\ell]$.

The proposed model contains four modules that are briefly described in the following. A mathematical formulation is provided in Section 2.1.

1. An en-route path choice model computes route-specific turning proportions at each gate, which are required to assign pedestrians to links. These turning proportions are computed based on prevailing traffic conditions and take into account the routes that are a priori known for each pedestrian.

2. For each link, a traffic flow model determines a sending capacity at the downstream end, and a receiving capacity at the upstream end. This is achieved by means of an empirical density-speed relation. The density on one link within a cell may have an influence on the walking speed on another, and vice versa. The sending capacity can be thought of as the maximum amount of users that may be sent to a next link in case of an unlimited outflow capacity and the receiving capacity as that which could be received by the link in case of an infinite traffic demand.

3. For each gate, a gate model determines which part of these sending and receiving capacities can potentially be sent, taking into account both up- and downstream constraints.

4. At cell level, a static capacity may be considered. Assume there exists a critical density k_c at which all pedestrian movement freezes. Then the static capacity of a cell ξ is defined as $M_\xi^{\mathsf{cap}} = k_c A_\xi$, representing the maximum number of pedestrians that can be present in the cell at any time.

2.1 Model formulation

The state of the model at any time interval τ is fully described by the number of pedestrians of each group ℓ on each link λ. This quantity is referred to as group-specific link occupation, and denoted by $M_{\lambda,\tau}^{\ell}$. Likewise, the total occupation on a link λ during time interval τ is denoted by $M_{\lambda,\tau}$.

The walking speed $V_{\lambda,\tau}$ on a link λ during time interval τ is given by the speed of the stream $V_{\sigma,\tau}$ it is associated with, i.e., $V_{\lambda,\tau} = V_{\sigma,\tau}$ if $\lambda \in \Lambda_\sigma$. Two

limit cases may be mentioned. If all edges of a cell ξ belong to the same stream ($|\Sigma_\xi| = 1$), an isotropic model results. If each link is characterized by its own stream ($|\Sigma_\xi| = |\Lambda_\xi|$), the number of streams is maximal. Xie and Wong (2014) propose to bundle links terminating in the same node as separate streams. This rule is adopted in the model specification presented in Section 3.

The number of pedestrians associated with a stream σ during time interval τ is given by

$$M_{\sigma,\tau} = \sum_{\lambda \in \Lambda_\sigma} M_{\lambda,\tau}. \tag{1}$$

The vector of stream occupations associated with cell ξ and time interval τ is denoted by $\mathbf{M}_{\xi,\tau} = [M_{\sigma,\tau}]$, with $\sigma \in \Sigma_\xi$. The vector $\mathbf{V}_{\xi,\tau} = [V_{\sigma,\tau}]$ represents the corresponding stream speeds.

For each cell ξ and time interval τ, a functional relation between the vector of stream occupations and the vector of stream speeds is assumed to exist. This relationship is referred to as stream-based fundamental diagram. In practice, time-invariant specifications are mostly used, presumably due to the difficult calibration of time-dependent models. If V_f represents the 'global' free-flow speed, the stream-based fundamental diagram may be expressed as

$$\mathbf{V}_{\xi,\tau} = V_f \mathbf{f}_{\xi,\tau}(\mathbf{M}_{\xi,\tau}). \tag{2}$$

Eq. (2) implies that pedestrians instantaneously adapt their speed with infinite acceleration if a change in occupation occurs. Moreover, it implies that all pedestrians obey the same density-speed relation, irrespective of the group they belong to. In principle, a multi-commodity framework would be possible (Cooper; 2014), which is subject to future research.

Regarding the functional form of the stream-based fundamental diagram, mainly two assumptions are made. These are inspired by Hughes' continuum theory for pedestrian flow (Hughes; 2002).

First, it is hypothesized that at zero cell occupation, the walking speed in any stream must be larger than zero, but may not exceed the global free-flow speed. If $f_{\sigma,\tau}$ represents the entry in $\mathbf{F}_{\xi,\tau}$ associated with stream $\sigma \in \Sigma_\xi$, this translates to

$$0 < f_{\sigma,\tau}(\mathbf{0}) \leq 1 \;\forall\; \sigma \in \Sigma_\xi, \xi \in \mathcal{X}, \tau \in \mathcal{T}, \tag{3}$$

where $\mathbf{0}$ represents the null vector of length $|\Sigma_\xi|$. The walking speed at

zero density can be lower than the global free-flow speed, which may be adequate for instance in uneven terrain.

Second, the fundamental diagram is assumed to be monotonically decreasing, i.e.,

$$\frac{\partial f_{\sigma,\tau}}{\partial M_{\sigma',\tau}} \leq 0 \;\forall\; \sigma, \sigma' \in \Sigma_\xi, \xi \in \mathcal{X}, \tau \in \mathcal{T}. \tag{4}$$

If a critical cell density k_c has been defined, it is further required that

$$f_{\sigma,\tau}(\mathbf{M}_{\xi,\tau}) = 0 \text{ if } \textstyle\sum_{\sigma\in\Sigma_\xi} M_{\sigma,\tau} = M_\xi^{\text{cap}}. \tag{5}$$

A sample specification of the fundamental diagram $\mathbf{f}_{\xi,\tau}(\mathbf{M}_{\xi,\tau})$ is provided in Section 3.

Intuitively, it may seem natural to require that pedestrians cannot traverse more than one link in a single time step. In numerical mathematics, this consideration is referred to as the Courant–Friedrichs–Lewy (CFL) condition. It can be expressed as

$$\Delta T \leq \frac{L_\lambda}{V_f},\; \forall\, \lambda \in \Lambda. \tag{6}$$

According to Eq. (6), the ratio of the shortest link length and the free-flow speed represents an upper bound for the discretization time step ΔT. Here, this bound is used to specify the time step, i.e.,

$$\Delta T = \min_{\lambda\in\Lambda}\{L_\lambda / V_f\}. \tag{7}$$

The actual choice of the time step within the bound specified by condition (6) is not critical for the stability of the model, but known to have an influence on numerical dispersion and computational cost (Daganzo; 1994).

Due to the decomposition of multi-directional flow into streams, on each link a uni-directional flow is prevalent. The magnitude of this flow is given by the hydrodynamic theory as the product of speed and density. Thus, on link $\lambda \in \Lambda_\sigma$ during time interval τ, the infinitesimal flow increment during an infinitesimal time interval dt may be expressed as

$$dQ_{\lambda,\tau} = \frac{M_{\lambda,\tau}}{L_\lambda} V_f f_{\sigma,\tau}(\mathbf{M}_{\xi,\tau})\, dt. \tag{8}$$

Based on Eq. (7), and by defining $L_{\text{min}} = \min_{\lambda\in\Lambda} L_\lambda$, the cumulative hydrodynamic flow on link λ during time interval τ can be defined as

$$\Delta Q_{\lambda,\tau} = \frac{L_{\text{min}}}{L_\lambda} M_{\lambda,\tau} f_{\sigma,\tau}(\mathbf{M}_{\xi,\tau}). \tag{9}$$

Due to properties (3) and (4), the function defined in Eq. (9) is known to reach a maximum $\Delta Q^{opt}_{\lambda,\tau}$ at a characteristic occupation $M^{opt}_{\lambda,\tau}$. For each link and time interval, this characteristic occupation divides the fundamental diagram into a free-flow and a congested regime. In the free-flow regime, an infinitesimal increase in occupation leads to an increased cumulative hydrodynamic flow. In the congested regime, inversely an increase in occupation leads to a decrease in flow.

The cumulative hydrodynamic link flow does not represent an actual flow, but one from which two characteristic quantities can be derived (Daganzo; 1995; Hänseler et al.; 2014). First, the hydrodynamic outflow capacity denotes the maximum number of pedestrians that can leave link λ during time interval τ according to the fundamental diagram. It is defined as equal to the cumulative hydrodynamic link flow $\Delta Q_{\lambda,\tau}$ if the actual occupation on the link is in the free-flow regime and set equal to $\Delta Q^{opt}_{\lambda,\tau}$ if it is in the congested regime, i.e.,

$$\Delta Q^{out}_{\lambda,\tau} = \begin{cases} \Delta Q_{\lambda,\tau} & \text{if } M_{\lambda,\tau} \leq M^{opt}_{\lambda,\tau}, \\ \Delta Q^{opt}_{\lambda,\tau} & \text{otherwise.} \end{cases} \tag{10}$$

Second, the hydrodynamic inflow capacity represents the maximum number of people that can enter link λ during time interval τ according to the fundamental diagram. It is equal to $\Delta Q^{opt}_{\lambda,\tau}$ in the free-flow regime and otherwise equal to the cumulative hydrodynamic cell flow $\Delta Q_{\lambda,\tau}$ in the congested regime, i.e.,

$$\Delta Q^{in}_{\lambda,\tau} = \begin{cases} \Delta Q^{opt}_{\lambda,\tau} & \text{if } M_{\lambda,\tau} \leq M^{opt}_{\lambda,\tau}, \\ \Delta Q_{\lambda,\tau} & \text{otherwise.} \end{cases} \tag{11}$$

Based on these definitions, the aforementioned modules of the propagation model can be formalized as follows:

I. En-route path choice model: Assuming that all pedestrians embarked on a given route have the same behavior, the turning proportion corresponding to the link sequence $\lambda \rightarrow \lambda'$ for the ensemble of people following route ρ that are on link λ during time interval τ may be denoted by $\delta^{\rho}_{\lambda\rightarrow\lambda',\tau}$. Since pedestrians are conserved, it holds that

$$\sum_{\lambda' \in \Theta^{\rho}_{\lambda}} \delta^{\rho}_{\lambda\rightarrow\lambda',\tau} = 1. \tag{12}$$

We assume there exist a traffic-dependent, group-specific potential field $P^{\ell}_{\lambda,\tau}$ and a functional relation that allows to infer turning proportions from it (Guo et al.; 2011). A sample specification is provided in Section 3.

II. Link model: The cumulative hydrodynamic inflow and outflow capacity are used to define the receiving and sending capacity, respectively. Unlike in the original CTM (Daganzo; 1995), these quantities are now link-, and not cell-specific.

The receiving capacity of link λ during time interval τ is equal to the cumulative hydrodynamic inflow capacity

$$R_{\lambda,\tau} = \Delta Q^{\text{in}}_{\lambda,\tau} \tag{13}$$

(a separate variable is defined only for notational consistency with the original CTM). Different from the original CTM, the static cell capacity M^{cap}_{ξ} is not taken into account by the receiving capacity, but considered by the cell model described further below.

The sending capacity from link λ to link $\lambda' \in \Theta^{\rho}_{\lambda}$ for pedestrian group ℓ during time interval τ is given by

$$S^{\ell}_{\lambda\to\lambda',\tau} = \delta^{\rho_\ell}_{\lambda\to\lambda',\tau} \min\left\{ M^{\ell}_{\lambda,\tau}, \frac{M^{\ell}_{\lambda,\tau}}{M_{\lambda,\tau}} \Delta Q^{\text{out}}_{\lambda,\tau} \right\}. \tag{14}$$

The first term in curly brackets ensures conservation of pedestrians, i.e., not more pedestrians may advance than are actually on the emitting link. The second term applies in case the hydrodynamic outflow capacity does not suffice to advance all pedestrians present on the link; then a demand-proportional supply distribution scheme is applied (Asano et al.; 2007). In that case, dispersion occurs, i.e., the group splits up in several fractions across links. Generally, dispersion is present on all except the shortest link, or whenever the prevailing speed is lower than the global free-flow speed.

III. Gate model: The gate model produces candidate transition flows from incoming to outgoing links. The number of users is thereby conserved.

Let the candidate inflow to link λ during time interval τ be given by

$$S_{\lambda,\tau} = \sum_{\lambda' \in \Phi^{o}_{\lambda}} \sum_{\ell \in \mathcal{L}} S^{\ell}_{\lambda' \to \lambda,\tau}. \tag{15}$$

The candidate transition flow from link λ to λ' during time interval τ associated with group ℓ may then be expressed as

$$Y^{\ell}_{\lambda \to \lambda',\tau} = \begin{cases} S^{\ell}_{\lambda \to \lambda',\tau} & \text{if } S_{\lambda',\tau} \leq R_{\lambda',\tau}, \\ \zeta^{\ell}_{\lambda \to \lambda',\tau} R_{\lambda',\tau} & \text{otherwise.} \end{cases} \tag{16}$$

If the candidate inflow to link λ' is inferior to the corresponding receiving capacity, the candidate transition flow is equal to the sending capacity. Otherwise, the flow disperses and again a demand-proportional supply distribution scheme is applied (Asano et al.; 2007), i.e.,

$$\zeta^{\ell}_{\lambda \to \lambda',\tau} = \frac{S^{\ell}_{\lambda \to \lambda',\tau}}{S_{\lambda',\tau}}. \tag{17}$$

In principle, gate models different from Eq. (16) can be envisaged. A variety of related models have been proposed in the literature dealing with multi-legged junctions in road networks (Daganzo; 1995; Lebacque; 1996; Jin and Zhang; 2003). These approaches seem however rather specific to the case of car traffic, and may not be directly applicable in the context of pedestrian flow.

IV. Cell model: If a static cell capacity M^{cap}_{ξ} is to be considered, this may be done at the cell level. Let the candidate inflow to cell ξ during time interval τ be given by

$$Y_{\xi,\tau} = \sum_{\lambda \in \Lambda_{\xi}} \sum_{\lambda' \in \Phi_{\lambda}} \sum_{\ell \in \mathcal{L}} Y^{\ell}_{\lambda' \to \lambda,\tau}. \tag{18}$$

The actual transition flow from link λ to $\lambda' \in \xi'$ during time interval τ associated with group ℓ can then be expressed as

$$G^{\ell}_{\lambda \to \lambda',\tau} = \begin{cases} Y^{\ell}_{\lambda \to \lambda',\tau} & \text{if } Y_{\xi',\tau} \leq M^{\text{cap}}_{\xi'} - M_{\xi',\tau}, \\ \eta^{\ell}_{\lambda \to \lambda',\tau} \left(M^{\text{cap}}_{\xi'} - M_{\xi',\tau} \right) & \text{otherwise.} \end{cases} \tag{19}$$

Again a demand-proportional supply distribution is proposed in case of insufficient static capacity, i.e.,

$$\eta^{\ell}_{\lambda\to\lambda',\tau} = \frac{Y^{\ell}_{\lambda\to\lambda',\tau}}{Y_{\xi',\tau}}. \tag{20}$$

In case no static cell capacity is to be considered, we have $M^{\text{cap}}_{\xi} \to \infty$, and it holds $G^{\ell}_{\lambda\to\lambda',\tau} \equiv Y^{\ell}_{\lambda\to\lambda',\tau}$.

At boundary cells, pedestrian source and sink terms need to be considered. The generation term for link λ during time interval τ associated with pedestrian group ℓ may be expressed as (Hänseler et al.; 2014)

$$W^{\ell}_{\lambda,\tau} = \begin{cases} X_{\rho_\ell,\tau_\ell} & \text{if } \lambda \in r^{\rho_\ell}_{o},\ \tau = \tau_\ell, \\ -M^{\ell}_{\lambda,\tau} & \text{if } \lambda \in r^{\rho_\ell}_{d}, \\ 0 & \text{otherwise.} \end{cases} \tag{21}$$

Newly added pedestrians that are unable to advance to a downstream link are retained in their origin cell until the traffic situation allows them to do so. Pedestrians reaching their destination are immediately cleared out. Source/sink and auxiliary cells ξ are assumed to have infinite capacity, and their link travel times are set to one, i.e., $L_\lambda/(V_\lambda \Delta T) = 1\ \forall\, \lambda \in \Lambda_\xi$.

If the demand and the initial state of the system, i.e., the group-specific occupation on all links, are known, the propagation of pedestrian groups along their routes can be computed by a difference scheme taking into account the actual transition flows and the generation terms defined in Eq. (19) and Eq. (21), i.e.,

$$M^{\ell}_{\lambda,\tau+1} = M^{\ell}_{\lambda,\tau} + \sum_{\lambda'\in\Phi^{\rho_\ell}_{\lambda}} G^{\ell}_{\lambda'\to\lambda,\tau} - \sum_{\lambda''\in\Theta^{\rho_\ell}_{\lambda}} G^{\ell}_{\lambda\to\lambda'',\tau} + W^{\ell}_{\lambda,\tau}. \tag{22}$$

Recursion (22) is independent of the processing order within a time interval (Daganzo; 1994). As shown by Hänseler et al. (2014), a non-dimensional model formulation may be obtained, minimizing the number of model parameters.

3 Model specification

In Section 2, the pedestrian fundamental diagram and the en-route path choice model have been left unspecified. A sample specification is provided in the following.

3.1 Pedestrian fundamental diagram

To illustrate the anisotropic features of the proposed DNL, the stream-based fundamental diagram developed by Xie and Wong (2014) is adopted. The key assumption in their approach lies in the interpretation of multi-directional flow as 'combinations of multiple pairs of bidirectional flows'. To identify pedestrians streams, Xie and Wong (2014) consider a static discretization of space, and group pedestrians walking towards the same edge within a cell as a 'copy of flow' (Potts and Oliver; 1972), i.e., as a single stream of pedestrians. For rectangular cells as in the case of Xie and Wong (2014), there are thus four prevalent streams, and for a triangular discretization there would be three.

In the framework of this work, the fundamental diagram proposed by Xie and Wong (2014) may be expressed as follows. Let $\phi_{\sigma,\sigma'}$ be the intersection angle between streams σ and σ' with $\phi_{\sigma,\sigma'} = 0$ if $\sigma = \sigma'$, and let α, β and ϑ denote model parameters. The occupation-dependent walking speed of stream $\sigma \in \Sigma_\xi$ is then given by the time-invariant relationship

$$V_\sigma = V_f \exp\left(-\vartheta \left(\frac{M_\xi}{A_\xi}\right)^2\right) \cdot \prod_{\sigma' \in \Sigma_\xi} \exp\left[-\beta \left(1 - \frac{V_\sigma M_\sigma}{V_\sigma M_\sigma + V_{\sigma'} M_{\sigma'}}\right)(1 - \cos \alpha\phi_{\sigma,\sigma'}) \frac{M_\sigma + M_{\sigma'}}{A_\xi}\right]. \quad (23)$$

Eq. (23) represents a generalization of Drake's one-dimensional traffic model (Drake et al.; 1967). The first exponential term considers the isotropic reduction in speed induced by the overall occupation in a cell. A large value of ϑ implies a strong reduction in walking speed with increasing occupation, and vice versa. The second term, i.e., the product of exponentials, represents the accumulation of pair-wise conflicting effects between streams. For that, both the flow ratio and the intersecting angle are considered. Involved in this term are two shape parameters α and β, for which no physical interpretation is given. Note that neither the first nor the second term considers the notion of a critical density. Instead of an upper bound on density, an exponential decrease in speed is assumed.

According to Eq. (23), the speed of a stream does not only depend on the magnitude of streams in the same cell, but also on their velocities. Determining the link speed in a n-dimensional stream field thus requires solving a system of n non-linear equations.

As stated by Xie and Wong (2014), specification (23) disposes of several key properties. Two of them are relevant in the context of this work. First, if a cell is nearly empty, the speed of any stream approaches the free-flow speed, i.e., $V_\sigma \to V_f$ when $M_\xi \to 0$. The speed of any stream is then independent of a change in occupation of any stream in the same cell, i.e., $\partial V_\sigma / \partial M_\sigma \to 0$ if $M_\xi \to 0$. Second, the model reduces to a one-dimensional Drake model if $\phi_{\sigma,\sigma'} = 0 \ \forall \sigma, \sigma' \in \Sigma_\xi$. Consequently, if the intersecting angle between two streams approaches zero, the conflicting effect vanishes.

Eq. (23) has been calibrated on trajectory data collected in a particularly busy pedestrian area in Hong Kong. Xie and Wong (2014) provide two similar parameter sets, which on average yield the following values: $V_f = 1.070$ m/s, $\alpha = 1.20$, $\beta = 0.132$ and $\vartheta = 0.065$ m^4.

3.2 En-route path choice model

The proposed en-route path choice model is based on the assumption of existence of a potential field from which local traffic-dependent and group-specific turning proportions can be computed. Inspired by Guo et al. (2011), the potential $P^\rho_{\gamma,\tau}$ is assumed to represent the remaining shortest distance from gate γ to the destination of route ρ at traffic conditions as they are prevalent during time interval τ. Assuming a logit-type model with parameter μ (Hänseler et al.; 2014), the choice fraction defined in Section 2.1 is given by

$$\delta^\rho_{\lambda\to\lambda',\tau} = \frac{\exp\left(-\mu P^\rho_{\gamma^d_{\lambda'},\tau}\right)}{\sum_{\lambda'\in\mathcal{O}^\rho_\nu} \exp\left(-\mu P^\rho_{\nu^d_{\gamma'},\tau}\right)}. \tag{24}$$

The fractions defined in Eq. (24) are memory-less in that the choice of the next link depends only on the current node, but not on the previous link, i.e., for any link $\lambda \in \mathcal{I}^\rho_\gamma$, it holds $\delta^\rho_{\lambda\to\lambda',\tau} = \tilde{\delta}^\rho_{\gamma\to\lambda',\tau}$. This property can be used to reduce the cost associated with the computation of these fractions.

We note that specification (24) is reactive, i.e., it does not yield an equilibrium solution (Huang et al.; 2009). Other specifications are obviously possible.

4 Test cases

By the time of submission, the computational model is fully developed and functional, but not yet validated. This validation is to be accomplished within a few weeks. Subsequently, several test cases are considered to examine and illustrate the behavior of the proposed loading model. These include counter- and cross-flow scenarios, as well as higher-dimensional flow patterns. A detailed sensitivity analysis with respect to model parameters is to be conducted, where particular emphasis is given to the anisotropic character of the model.

5 Case study

Trajectory data from a real case study is available, from which demand and walking times can be extracted. Based on this data, the ability of the proposed model to reproduce empirically observed behavior can be studied. In particular, the difference in performance as compared to an isotropic loading model may be investigated.

6 Conclusions

A pedestrian network loading model for time-dependent, multi-directional and congested pedestrian flow has been outlined. A computational model has been implemented and is to be validated. By the time of the conference, the analysis of several test cases, as well as of a real case study is envisaged.

A Computation of fundamental diagram

This section discusses the numerical computation of the fundamental diagram specified in Section 3. In the following, the dependency of time is omitted for improved readability.

Let the stream density be given by

$$m_\sigma = M_\sigma / A_\xi, \tag{25}$$

with $\mathbf{m}_\xi = [m_\sigma]$, $\sigma \in \Sigma_\xi$, denoting the vector grouping the densities of streams associated with cell ξ. Accordingly, a non-dimensional velocity is defined as

$$v_\sigma = V_\sigma / V_f, \tag{26}$$

with $\mathbf{v}_\xi = [v_\sigma]$ the corresponding vector grouping the non-dimensional stream velocities. Moreover, a function

$$g_{\sigma,\sigma'}(\mathbf{m}_\xi, \mathbf{v}_\xi) = \tilde{\beta}_{\sigma,\sigma'}(\mathbf{m}_\xi) \frac{v_{\sigma'} m_{\sigma'}}{v_\sigma m_\sigma + v_{\sigma'} m_{\sigma'}}, \tag{27}$$

as well as the parameters

$$\tilde{\vartheta}(\mathbf{m}_\xi) = \vartheta m_\xi^2 \tag{28}$$

are defined, where the total cell density is given by $m_\xi = \sum_{\sigma \in \Sigma_\xi} m_\sigma$, and

$$\tilde{\beta}_{\sigma,\sigma'}(\mathbf{m}_\xi) = \beta \left(1 - \cos\left(\alpha \phi_{\sigma,\sigma'}\right)\right) (m_\sigma + m_{\sigma'}). \tag{29}$$

A root-finding problem equivalent to Eq. (23) can then be formulated as

$$h_\sigma(\mathbf{m}_\xi, \mathbf{v}_\xi) = 0, \tag{30}$$

where

$$h_\sigma(\mathbf{m}_\xi, \mathbf{v}_\xi) = \log(v_\sigma) + \tilde{\vartheta}(\mathbf{m}_\xi) + \sum_{\sigma' \in \Sigma_\xi, \sigma' \neq \sigma} g_{\sigma,\sigma'}(\mathbf{v}_\xi). \tag{31}$$

For any stream density vector $\mathbf{m}_\xi$, the vector of non-dimensional stream velocities $\mathbf{v}_\xi$ is thus given by the unique root of Eq. (31).

The partial derivatives of the functions defined in Eq. (27) and Eq. (31) are

$$\frac{\partial h_\sigma}{\partial x_\sigma} = \frac{1}{x_\sigma} + \sum_{\sigma' \in \Sigma, \sigma' \neq \sigma} \frac{\partial g_{\sigma,\sigma'}}{\partial x_\sigma} \tag{32}$$

and

$$\frac{\partial h_\sigma}{\partial x_{\sigma'}} = \frac{\partial g_{\sigma,\sigma'}}{\partial x_{\sigma'}}, \tag{33}$$

as well as

$$\frac{\partial g_{\sigma,\sigma'}}{\partial x_\sigma} = -\beta_{\sigma,\sigma'}(\mathbf{m}) \frac{m_\sigma m_{\sigma'} x_{\sigma'}}{(m_\sigma x_\sigma + m_{\sigma'} x_{\sigma'})^2} \tag{34}$$

and

$$\frac{\partial g_{\sigma,\sigma'}}{\partial x_{\sigma'}} = \beta_{\sigma,\sigma'}(\mathbf{m}) \frac{m_\sigma m_{\sigma'} x_\sigma}{(m_\sigma x_\sigma + m_{\sigma'} x_{\sigma'})^2}, \tag{35}$$

respectively.

We note that the optimal occupation associated with Eq. (23) for unidirectional flow is given by

$$M_\sigma^{\mathrm{opt,1d}} = A_\xi / \sqrt{2\vartheta}, \tag{36}$$

for which a velocity of

$$V_\sigma^{\mathrm{opt,1d}} = V_f \exp(-1/2) \tag{37}$$

is obtained. These values are useful in the numerical optimization routines, notably to estimate initial values.

A.1 Actual stream velocities

For a given vector of stream occupations $\mathbf{m}_\xi$, the corresponding stream velocities $\mathbf{v}_\xi$ can be obtained by solving the coupled fixed-point problem defined by Eq. (30) for the set of streams Σ_ξ. For this task, in this work the Marquardt-Levenberg algorithm is used, for which the Jacobian is computed analytically using Eq. (32) and Eq. (33).

A.2 Optimal stream occupation and velocity

To compute the hydrodynamic inflow and outflow capacities, for each link $\lambda \in \Lambda$ the optimal cumulative flow $\Delta Q_{\lambda,\tau}^{\mathrm{opt}}$, and the corresponding optimal link occupation $M_{\lambda,\tau}^{\mathrm{opt}}$ need to be known. They are obtained in two steps. First, for each stream $\sigma \in \Sigma_\xi$, the optimal occupation and velocity are computed. Then, these occupations are assigned to the corresponding links that are associated with the stream.

To determine the optimal density m_σ^{opt} and speed v_σ^{opt} of a stream $\sigma \in \Sigma_\xi$, the density $m_{\sigma'}$ and speed $v_{\sigma'}$ of all other streams $\sigma' \in \Sigma_\xi$, $\sigma' \neq \sigma$,

are assumed to be known, i.e., the actual densities and velocities (see Section A.1) are used. Let the corresponding vectors be denoted by $\mathbf{m}'_\xi$ and $\mathbf{v}'_\xi$, respectively. The optimization problem then consists in finding

$$m_\sigma^{opt} = \arg\max_{m \geq 0} m v_\sigma(m; \mathbf{m}'_\xi, \mathbf{v}'_\xi) \tag{38}$$

where v_σ is implicitly given by

$$h_\sigma(m_\sigma, v_\sigma; \mathbf{m}'_\xi, \mathbf{v}'_\xi) = 0. \tag{39}$$

Given the optimal density of a stream, the corresponding optima for links are obtained from a homogeneous distribution scheme. Specifically, the optimal occupation of link $\lambda \in \Lambda_\sigma$ is assumed to be given by

$$M_{\lambda,\tau}^{opt} = \frac{1}{|\Lambda_\sigma|} M_{\sigma,\tau}^{opt}. \tag{40}$$

Defining the non-dimensional link length as $l_\lambda = L_\lambda / L_{min}$, the hydrodynamic flow capacity of a link $\lambda \in \Lambda_\sigma$ is then given by

$$\Delta Q_{\lambda,\tau}^{opt} = \frac{1}{l_\lambda} M_{\lambda,\tau}^{opt} \frac{v_{\lambda,\tau}^{opt}}{v_f}. \tag{41}$$

Specification (40) represents a heuristic choice that has proven useful for the illustration of the model. Alternative formulations may of course be considered.

References

Abdelghany, A., Abdelghany, K., Mahmassani, H. S. and Al-Zahrani, A. (2012). Dynamic simulation assignment model for pedestrian movements in crowded networks, *Transportation Research Record: Journal of the Transportation Research Board* **2316**(1): 95–105.

Asano, M., Sumalee, A., Kuwahara, M. and Tanaka, S. (2007). Dynamic cell transmission-based pedestrian model with multidirectional flows and strategic route choices, *Transportation Research Record: Journal of the Transportation Research Board* **2039**(1): 42–49.

Blue, V. J. and Adler, J. L. (2001). Cellular automata microsimulation for modeling bi-directional pedestrian walkways, *Transportation Research Part B: Methodological* **35**(3): 293–312.

Cheung, C. Y. and Lam, W. H. K. (1998). Pedestrian route choices between escalator and stairway in MTR stations, *Journal of Transportation Engineering* **124**(3): 277–285.

Cooper, G. A. (2014). *A multi-class framework for a pedestrian cell transmission model accounting for population heterogeneity*, Master's thesis, Ecole Polytechnique Fédérale de Lausanne.

Daamen, W. (2004). *Modelling passenger flows in public transport facilities*, PhD thesis, Delft University of Technology.

Daamen, W., Bovy, P. H. L. and Hoogendoorn, S. P. (2005). Influence of changes in level on passenger route choice in railway stations, *Transportation Research Record: Journal of the Transportation Research Board* **1930**(1): 12–20.

Daganzo, C. F. (1994). The cell transmission model: A dynamic representation of highway traffic consistent with the hydrodynamic theory, *Transportation Research Part B: Methodological* **28**(4): 269–287.

Daganzo, C. F. (1995). The cell transmission model, Part II: Network traffic, *Transportation Research Part B: Methodological* **29**(2): 79–93.

Drake, J. S., Schofer, J. L. and May, A. D. (1967). A statistical analysis of speed-density hypotheses, *Proceedings of the Third International Symposium on the Theory of Traffic Flow*, New York, pp. 112–117.

Duives, D. C., Daamen, W. and Hoogendoorn, S. P. (2013). State-of-the-art crowd motion simulation models, *Transportation Research Part C: Emerging Technologies* **37**(12): 193–209.

Guo, R. Y., Huang, H. J. and Wong, S. C. (2011). Collection, spillback, and dissipation in pedestrian evacuation: A network-based method, *Transportation Research Part B: Methodological* **45**(3): 490–506.

Hänseler, F. S., Bierlaire, M., Farooq, B. and Mühlematter, T. (2014). A macroscopic loading model for time-varying pedestrian flows in public walking areas, *Transportation Research Part B: Methodological* **69**: 60 – 80.

Hänseler, F. S., Molyneaux, N. A. and Bierlaire, M. (2015). Schedule-based estimation of pedestrian origin-destination demand in railway stations, *TRANSP-OR Report Nr. 150108*, Ecole Polytechnique Fédérale de Lausanne.

Helbing, D. and Molnár, P. (1995). Social force model for pedestrian dynamics, *Physical review E* **51**(5): 4282–4286.

Hoogendoorn, S. P. and Bovy, P. H. L. (2004). Pedestrian route-choice and activity scheduling theory and models, *Transportation Research Part B: Methodological* **38**(2): 169–190.

Huang, L., Wong, S. C., Zhang, M., Shu, C. W. and Lam, W. H. K. (2009). Revisiting Hughes' dynamic continuum model for pedestrian flow and the development of an efficient solution algorithm, *Transportation Research Part B: Methodological* **43**(1): 127–141.

Hughes, R. L. (2002). A continuum theory for the flow of pedestrians, *Transportation Research Part B: Methodological* **36**(6): 507–535.

Jin, W. L. and Zhang, H. M. (2003). On the distribution schemes for determining flows through a merge, *Transportation Research Part B: Methodological* **37**(6): 521–540.

Kaakai, F., Hayat, S. and El Moudni, A. (2007). A hybrid Petri nets-based simulation model for evaluating the design of railway transit stations, *Simulation Modelling Practice and Theory* **15**(8): 935–969.

Kallas, S. (2014). Railways: Paving the way for more growth, more efficiency and service quality in Europe, *Press release 14*, European Commission for Transport, Brussels, Belgium.

Lam, W. H. K., Lee, J., Chan, K. S. and Goh, P. K. (2003). A generalised function for modeling bi-directional flow effects on indoor walkways in Hong Kong, *Transportation Research Part A: Policy and Practice* **37**(9): 789–810.

Lam, W. H. K., Lee, J. Y. S. and Cheung, C. Y. (2002). A study of the bi-directional pedestrian flow characteristics at Hong Kong signalized crosswalk facilities, *Transportation* **29**(2): 169–192.

Lebacque, J.-P. (1996). The Godunov scheme and what it means for first order traffic flow models, *International Symposium on Transportation and Traffic Theory*, pp. 647–677.

Lee, J. Y. S., Lam, W. H. K. and Wong, S. C. (2001). Pedestrian simulation model for Hong Kong underground stations, *Intelligent Transportation Systems*, IEEE, pp. 554–558.

Lighthill, M. J. and Whitham, G. B. (1955). On kinematic waves. II. A theory of traffic flow on long crowded roads, *Proceedings of the Royal Society of London. Series A. Mathematical and Physical Sciences* **229**(1178): 317–345.

Potts, R. B. and Oliver, R. M. (1972). *Flows in transportation networks*, Academic Press, New York.

Richards, P. I. (1956). Shock waves on the highway, *Operations Research* **4**(1): 42–51.

Robin, T., Antonini, G., Bierlaire, M. and Cruz, J. (2009). Specification, estimation and validation of a pedestrian walking behavior model, *Transportation Research Part B: Methodological* **43**(1): 36–56.

Seer, S., Bauer, D., Brandle, N. and Ray, M. (2008). Estimating pedestrian movement characteristics for crowd control at public transport facilities, *Intelligent Transportation Systems*, IEEE, pp. 742–747.

Weidmann, U. (1992). *Transporttechnik der Fussgänger*, Schriftenreihe des IVT Nr. 90, Institute for Transport Planning and Systems, ETH Zürich, Switzerland.

Wong, S. C., Leung, W. L., Chan, S. H., Lam, W. H. K., Yung, N. H. C., Liu, C. Y. and Zhang, P. (2010). Bidirectional pedestrian stream model with oblique intersecting angle, *Journal of Transportation Engineering* **136**(3): 234–242.

Xie, S. and Wong, S. C. (2014). A Bayesian Inference Approach to the Development of a Multidirectional Pedestrian Stream Model, *Transportmetrica A: Transport Science* (forthcoming): 1–16.

Yperman, I. (2007). *The link transmission model for dynamic network loading*, PhD thesis, Katholieke Universiteit Leuven.